FEATURED ARTICLE

Two-stage Bayesian GWAS of 9576 individuals identifies SNP regions that are targeted by miRNAs inversely expressed in Alzheimer's and cancer

Gita A. Pathak[1] | Zhengyang Zhou[2] | Talisa K. Silzer[1] | Robert C. Barber[3] | Nicole R. Phillips[1] | for the Alzheimer's Disease Neuroimaging Initiative, Breast and Prostate Cancer Cohort Consortium, and Alzheimer's Disease Genetics Consortium*

[1]Department of Microbiology, Immunology and Genetics, Graduate School of Biomedical Sciences, University of North Texas Health Science Center, Fort Worth, Texas, USA

[2]Department of Biostatistics and Epidemiology, School of Public Health, University of North Texas Health Science Center, Fort Worth, Texas, USA

[3]Department of Pharmacology & Neuroscience, Graduate School of Biomedical Sciences, University of North Texas Health Science Center, Fort Worth, Texas, USA

Correspondence
Nicole R. Phillips, Assistant Professor, CBH—327, Department of Microbiology, Immunology and Genetics, Graduate School of Biomedical Sciences, University of North Texas Health Science Center, Fort Worth, TX 76107, USA.
Email: Nicole.Phillips@unthsc.edu

*Data used in preparation of this article were obtained from the Alzheimer's Disease Neuroimaging Initiative (ADNI) database (adni.loni.usc.edu), Breast and Prostate Cancer Cohort Consortium (BPC3), and the Alzheimer's Disease Genetics Consortium (ADGC). As such, the investigators within each organization contributed to the design and implementation of ADNI, BPC3, and ADGC and/or provided data but did not participate in analysis or writing of this report. A complete listing of ADNI investigators can be found at http://adni.loni.usc.edu/wp-content/uploads/how_to_apply/ADNI_Acknowledgement_List.pdf

Abstract

Introduction: We compared genetic variants between Alzheimer's disease (AD) and two age-related cancers—breast and prostate —to identify single-nucleotide polymorphisms (SNPs) that are associated with inverse comorbidity of AD and cancer.

Methods: Bayesian multinomial regression was used to compare sex-stratified cases (AD and cancer) against controls in a two-stage study. A ± 500 KB region around each replicated hit was imputed and analyzed after merging individuals from the two stages. The microRNAs (miRNAs) that target the genes involving these SNPs were analyzed for miRNA family enrichment.

Results: We identified 137 variants with inverse odds ratios for AD and cancer located on chromosomes 19, 4, and 5. The mapped miRNAs within the network were enriched for miR-17 and miR-515 families.

Discussion: The identified SNPs were rs4298154 (intergenic), within *TOMM40/APOE/APOC1*, *MARK4*, *CLPTM1*, and near the *VDAC1/FSTL4* locus. The miRNAs identified in our network have been previously reported to have inverse expression in AD and cancer.

KEYWORDS

aging, Alzheimer's, cancer, *CLPTM1*, *FSTL4*, genetic risk, GWAS, inverse association, *MARK4*, two-stage Bayesian, *VDAC1*

1 | INTRODUCTION

The aging population, defined as 65 years or older, is expected to experience a substantial demographic shift. By the year 2060, this group is expected to reach 98 million in the United States, placing an unprecedented burden on the health-care system.[1] Due to the role of aging in accumulation of physiological deterioration, the number of chronic diseases affecting this population continues to rise and many individuals suffer the co-occurrence of two or more diseases (ie, comorbidity).[2] In contrast to the coexistence of diseases, some chronic age-associated diseases have been identified to be inversely comorbid—a lower-than-expected occurrence of the secondary disease after the index/first

diagnosis.[3] These intriguing inverse associations between select diagnoses have garnered much attention in the last few years, as they shed light on the heterogeneity of age-associated multifactorial diseases.

Alzheimer's disease (AD) and cancer are two predominant age-associated diseases that are inversely comorbid as reported by several epidemiological findings. In a meta-analysis of association studies from 1966 to 2013, AD patients had a decreased incidence of cancer by 42% and individuals with cancer history had 37% reduced risk of AD.[4] In a recent retrospective study of >3 million U.S. veterans, cancer survivors aged ≥65 years had a lower risk of AD than other age-related outcomes. The odds ratio was 0.89 in 14 cancer types after excluding melanoma, prostate, and colorectal cancer.[5] These findings have fueled numerous exploratory investigations into possible genetic mechanisms that may be responsible for this inverse association between two common age-related diseases.

While genome-wide association studies (GWAS) have identified multiple genetic loci contributing to either AD or cancer, no study has reported cross-phenotypic effects of individual genetic variants.[6–8] Therefore, we sought to detect variants that confer inverse risk for AD and cancer by (1) harmonizing the intermediate risk factor—age, between the two disease populations, and (2) directly comparing cases which represent the two extremes of phenotypic variance to a common set of controls. The comparison of multiple cases to controls (also known as cross-disorder studies) warrants the use of multinomial logistic regression as it provides flexible framework to compare and explore genetic relationships between these different phenotypes.[9] In this article, our goal is to test the relationship between AD and cancer in a conservative setting of no single-nucleotide polymorphism (SNP) effect exists between the two diseases, and we aimed to address this goal by conducting a Bayesian multinomial GWAS (B-GWAS) to identify genetic variants that confer inverse risk in the aging population between 60 and 80 years for AD and cancer, using the two most prevalent age-related cancers: breast cancer and prostate cancer.[10] Unlike frequentist approaches, which use *P*-values to draw statistical inference in GWAS, B-GWAS uses Bayes factor to provide the strength of the association evidence for each genetic locus.[11,12] Multiple GWAS scenarios such as fine-mapping of variants,[13] pleiotropic and regulatory variants use Bayesian methods in genome-wide studies to achieve higher accuracy and prediction than frequentist approach.[14] We conducted a B-GWAS in two phases—discovery and replication—comparing AD and cancer to common controls. All datasets were stratified by sex and harmonized on age. Replicated hits were further investigated in the merged dataset (discovery and replication) via B-GWAS of imputed genotypes within 1Mbp window (±500 KB) of each hit, and conditional analysis was used to identify secondary hits.

2 | METHODS AND MATERIALS

2.1 | Data description

We obtained access to datasets from Alzheimer's Disease Genetics Consortium (ADGC) (phs000372.v1.p1)[15] and Breast Prostate

RESEARCH IN CONTEXT

1. Systematic review: Multiple epidemiological studies have reported an inverse relationship between Alzheimer's disease (AD) and cancer. However, single-nucleotide polymorphism (SNP) studies investigating this relationship have used genome-wide association studies (GWAS) summary statistics and combined cancers.

2. Interpretation: We found individual-level SNPs to confer inverse odds ratio between AD and prostate and breast cancer. We found a total of 137 variants; 21 variants on chromosome 4 comparing prostate cancer and AD in 6258 males. In 3318 females comparing breast cancer and AD against controls, we found 113 significant variants on chromosome 19 and three variants on chromosome 5.

3. Future direction: Our findings identify SNPs with cross-phenotypic effects. Micro RNAs (miRNAs) targeting the implicated regions have been reported to have inverse expression between AD and cancer. These markers have the potential to become genetic and blood-based biomarkers, warranting simultaneous investigation in both AD and cancer. Our future work will compare regulatory SNPs associated with AD and cancer.

HIGHLIGHTS

- Single-nucleotide polymorphisms (SNPs) exhibit cross-phenotypic odds ratios between Alzheimer's disease (AD) and cancer.
- Genes containing/proximate to these SNPs are targets of micro RNAs (miRNAs) that are inversely expressed between AD and cancer.
- The miR-515 and -17 families were enriched among the miRNAs gene network.

Cancer Care Consortium (BPC3) (phs000812.v1.p1)[16] via the database of Genotypes and Phenotypes (dbGaP)'s authorized application to individual-level genotype data. We also obtained access to Alzheimer's Disease Neuroimaging Initiative (ADNI) (www.adni-info.org) (see Supplementary file3—Text S1 in supporting information for details). These datasets were chosen because all samples were genotyped on the same platform—Illumina Human660W-Quad—to minimize any technical bias and harmonization issues while merging the datasets and potential array-specific inaccuracies during imputation. The research protocol for this project was reviewed by University of North Texas Health Science Center Institutional Review Board on June 24, 2016, and determined to be exempt human subject research under IRB–2016-090.

The first cohort in the BPC3 dataset[16]—phs00812.BreastProstateCancer.v1.p1.c1 (BPC3-c1)—had a total of 4915 participants. There were 2314 individuals in the prostate cancer group with genotype data for 583,132 SNPs. The total number of individuals in the breast cancer group was 2601 with genotyped data of 541,219 SNPs. The second cohort in BPC3—phs00812.BreastProstateCancer.v1.p1.c4 (BPC3-c4)—had 4664 participants. The total number of individuals in the prostate cancer group in this cohort was 4069 with genotype data for 583,132 SNPs. The total number of individuals in the breast cancer group was 595 with genotyped data of 541,219 SNPs on hg18 build. The ADGC dataset[15] had genetic variant data of 6065 individuals genotyped on the Illumina platform via Human660WQuad array. The ADC1 dataset had 2905 individuals with 657,366 genotyped markers, and the ADC2 dataset had 1170 individuals with 657,366 genotyped markers on hg19 build. We combined these two datasets for the final ADGC dataset. From the ADNI cohort, we used the ADNI-1 dataset as it was also genotyped on Illumina Human660W-Quad array. The ADNI-1 dataset had 757 individuals with 620,902 typed SNP markers.

2.2 | Merging and quality control of datasets

For the discovery stage, we merged individual-level genotype data from ADGC and BPC3 (c1) by aligning strand and genomic build to hg19 using PLINK (v1.9).[17] A total of 8990 individuals (self-described European ancestry) remained in the merged dataset with 539,774 common genotyped SNPs. We then followed quality control protocol outlined by Anderson et al.;[18] principal components were calculated using R package "SNPRelate."[19] After quality control (QC) in discovery phase, 5350 individuals (females: 2672, males: 2678) and 539,774 SNPs remained.

For the replication stage, we merged individual-level genotype data from ADNI and BPC3 (c4) by harmonizing strand using the array manufacturer's documentation and converted to genomic build hg19. After QC, 486,308 markers in 4226 individuals remained. This QC'd dataset was stratified on sex, with 3580 males and 646 females. Details of QC protocol and number of individuals removed at each stage are outlined in Supplementary file3 FigureS2 in supporting information.

2.3 | Bayesian multinomial genome-wide association studies

For the discovery stage, we conducted B-GWAS adjusted for age, and ancestry—principal components (PCs) 1–10 (self-described as Caucasian/European ancestry)—using Trinculo[20] with the default prior parameter. The variance proportion for each of the first three PCs was <2% for each dataset. There was no significant difference ($P > 0.05$) in means of eigenvalues between phenotypes after the first three PCs; calculated in EIGENSTRAT[21] for both stages of datasets. We compared 896 males with AD and 997 males with prostate cancer to a combined

male control population of 785 individuals from the two datasets. Similarly, we conducted B-GWAS in females, comparing 942 females with AD and 460 females with breast cancer to a combined female control population of 1270 individuals. We selected SNPs that were significant with a joint log Bayes factor ≥ 3 and odds ratio (OR) in the opposite direction for the two diseases (OR_AD > 1 and OR_breast/prostate < 1 or OR_AD < 1 and OR_breast/prostate > 1). Next, in a replication phase, these top significant variants were analyzed in independent sample sets. Consideration of significance threshold and comparison to P-values was motivated by works of Dr. Wakefield.[11,22]

For the replication stage, we followed the same QC protocol, comparing 149 males with AD, and 1046 males with prostate cancer, to a combined control male population of 2385 individuals. Correspondingly, association analysis was performed in 107 females with AD and 229 females with breast cancer to a combined female control population of 310 individuals.

2.4 | Regional genome-wide association studies

Imputation was performed using IMPUTE2[23] with a 1000 genomes Phase 3 dataset for each of significant hit regions. The datasets from the two stages were merged for a 1Mbp region (± 500 KB) of the replicated hits that were identified in the B-GWAS. Following SNP-level QC, we performed a regional GWAS in 6258 males comparing AD and prostate cancer against controls on chromosome 4. Similarly, following QC, we performed regional GWAS in 3318 females comparing AD and breast cancer against common controls on chromosomes 19 and 5. For the regional GWAS on chromosome 19, we identified haploblocks of the 1Mbp region using plink v1.9. There were four *TOMM40* haploblocks of 21, 6, 2, and 11 SNPs and one *APOE* haploblock containing six SNPs. To identify higher risk SNPs between *TOMM40* and *APOE*, a total of four separate haploblock-based associations were conducted merging each of the *TOMM40* and *APOE* haploblocks, keeping only individuals with all SNPs (no missing data). To identify secondary hits on chromosome 19, conditional tests were performed using *APOE* SNPs—rs429358 and rs769449. For other regions, the top two significant SNPs were used to perform conditional analysis.

2.5 | SNP annotations and testing for enriched processes

All significant SNPs were mapped to genes using Ensembl's Ch37 Variant Effect Predictor (http://grch37.ensembl.org/Homo_sapiens/Tools/VEP), and functional annotations were retrieved from SNP nexus.[24] Figures were plotted using ggplot2, gene annotations were visualized with Gviz package, and a linkage disequilibrium (LD) map was created using LDheatmap package in R. The mapped genes were tested for functional and diseases processes and visualized using Ingenuity Pathway Analysis (QIAGEN Inc., https://www.qiagenbioinformatics.com/products/ingenuity-pathway-analysis).

2.6 | miRNA enrichment analysis and text mining for miRNA expression

All the annotated significant genes were used as input in miRNet.[25] The miRNA nodes in network were filtered on degree filter of 1.0, to reduce orphan miRNAs. The filtering prioritizes miRNAs with at least two connecting query genes. The miRNAs in the network were then assessed for miRNA family enrichment using a hypergeometric test, with a P-value < 0.05 considered significant.

3 | RESULTS

3.1 | B-GWAS in sex-stratified Alzheimer's disease and cancer

We found 391 SNPs to be significant as shown in the bokeh plot (Figure 1, top panel) by comparing control males with males with AD and males with prostate cancer (Supplementary file 1 Table S1). Similarly, we tested the relationship of AD and breast cancer, by comparing females with AD, and females with breast cancer against female controls, which resulted in 287 significant loci (Supplementary file 1 Table S3 in supporting information) with inverse ORs between AD and breast cancer (Figure 1, bottom panel).

We evaluated these top significant SNP loci in another dataset of individuals, merging Alzheimer's population of ADNI-1, and breast and prostate cancer population of BPC3 (c4) followed by QC procedures. The QC'd dataset was then separated by sex. In this replication stage, out of 391 significant SNPs from the discovery stage, 381 SNPs were present in the replication dataset (Figure 2, top panel). The association analysis, adjusted for age and PCs 1-10, revealed one SNP that replicated in this dataset—SNP_allele: rs4298154_C an intergenic SNP on chromosome 4, had the odds ratio of 0.775 for AD (logBF—1.9) and 1.25 for prostate cancer (logBF—3.7) with an overall logBF of 5.14 (Supplementary file 1 Table S2 in supporting information).

In females, out of 287 significant SNPs from the discovery stage, 274 were present in the replication stage. The association test replicated two significant loci (Supplementary file 1 Table S4 in supporting information): (1) rs2075650_A had odds ratio of 0.52 for AD (logBF—13.418) and 1.245 for breast cancer (logBF—3.17), with an overall logBF of 14.458; (2) rs17700949_A, mapped on chromosome 5 near *C5orf15* and voltage-dependent anion channel 1 (*VDAC1*) gene, had odds ratio of 0.817 for AD (logBF—1.74) and 1.256 for breast cancer (logBF—2.483), with an overall logBF of 3.33 (Figure 2, bottom panel).

3.2 | Regional B-GWAS of replicated SNP hits and conditional analysis

To achieve finer SNP resolution, a 1Mbp region was imputed around the replicated hits (±500 KB), hereafter referred to as "risk region" in each dataset. The two datasets for this risk region analysis were merged to improve power by increasing sample size. Following SNP-level QC, a regional B-GWAS with default prior and adjustment for age and PCs 1–10 from the merged datasets was performed in 6258 males comparing AD and prostate cancer against controls on chromosome 4. For the risk region in chromosome 4, a total of 3107 variants were analyzed by B-GWAS and 21 SNPs were found to be significant (Supplementary file 1 Table S5 in supporting information), the most significant SNPs were (1) rs4298154_C having odds ratio of 0.813 and 1.223 for AD and prostate cancer, respectively, with overall logBF of 10.65; and (2) rs57139228_G having odds ratio of 0.888 and 1.155 for AD and prostate cancer, respectively, with overall logBF of 5.41 (Figure 3). After conditioning on these hits, no SNPs remained significant.

Similarly, regional B-GWAS was performed in 3318 females comparing AD and breast cancer against common controls on chromosomes 19 and 5. Of 1499 variants in the risk region on chromosome 19, 113 SNPs were found to be significant (Supplementary file 1 Table S6 in supporting information). The top significant SNPs were (1) rs34404554_C having odds ratios of 0.321 and 1.193 for AD and breast cancer, respectively, with overall logBF of 179.46; (2) rs71352238_T with odds ratio of 0.32 and 1.2 for AD and breast cancer, respectively, with overall logBF of 178.81; and (3) rs2075650 having odds ratio of 0.325 and 1.178 for AD and breast cancer, respectively, with overall logBF of 175.59. All three SNPs were mapped to *TOMM40*. Select top significant SNPs are labeled in Figure 4 (left panel). To identify which SNPs between *TOMM40* and *APOE* were most significant, we conducted association with SNPs in each haploblock of *TOMM40* and *APOE* keeping individuals who had a complete set of SNPs. Here, we found that *APOE* SNPs were more significant than *TOMM40*, and after conditioning on the top two *APOE* SNPs, none of the *TOMM40* were significant for both diseases; significance was observed only for AD (logBF > 1.5). Because the *TOMM40* SNPs were not independent of *APOE* we conditioned the association analysis using *APOE* SNPs—rs429358 and rs769449. After conditioning, none of the SNPs were significant for both diseases.

The second replicated hit between AD and breast cancer was in chromosome 5; we analyzed 2340 SNPs in this 1Mb region for inverse association. A total of three SNPs remained significant including the replicated hit (1) rs17700949_A having odds ratios of 0.873 (logBF—4.24) and 1.174 (logBF—4.54) for AD and breast cancer, respectively, with overall logBF of 6.18; (2) rs10068691_G having odds ratios of 1.13 (logBF—2.75) and 0.89 (logBF—2.17) for AD and breast cancer, respectively, with overall logBF of 3.24; and (3) rs1109309_G having odds ratio of 0.896 (logBF—2.54) and 1.136 (logBF—2.75) for AD and breast cancer, respectively, with overall logBF of 3.48 (Figure 4, right panel; Supplementary file 1 Table S7 in supporting information). All three SNPs are in close proximity to one another and mapped to an intergenic region between follistatin like 4 (*FSTL4*) and *VDAC1* based on GRCh37/hg19.

The significant SNPs in the regional B-GWAS of AD and prostate cancer on chromosome 4 are in the intergenic region, and the nearby genes are *ARAP2*, *DTHD1*, and *KIAA1239*. Additionally, annotation was retrieved from the Genetic Association Database using SNP-nexus, which showed association of these SNPs with *HTRA3*, *AREG*, and *NRAS* (Supplementary file2). Interestingly, some of the variants in this
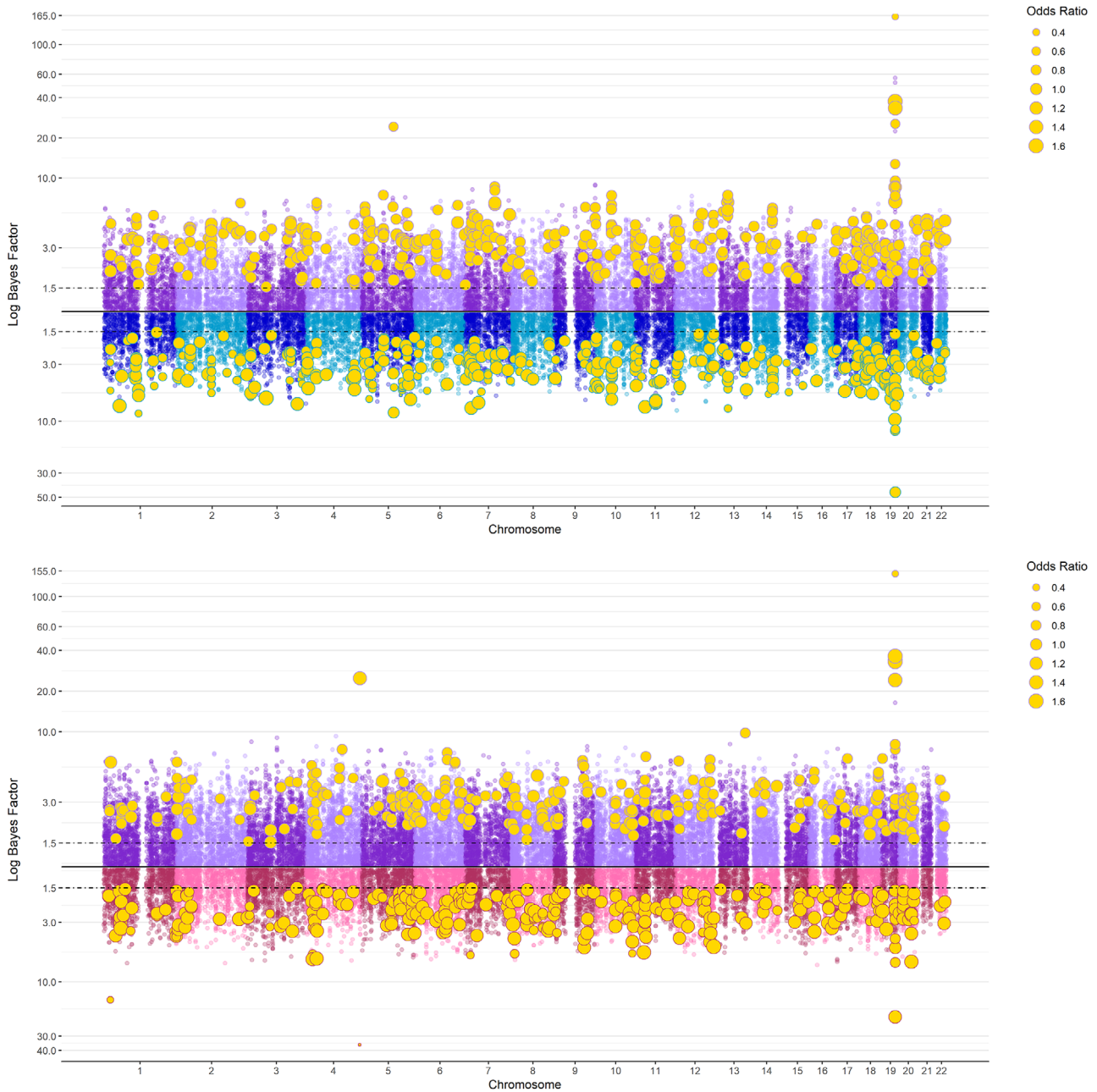
FIGURE 1 Discovery phase B-GWAS results. Top panel: Bokeh plot of multinomial GWAS comparing Alzheimer's disease (AD) and prostate cancer in the discovery stage. The purple Manhattan plot shows the results from AD versus control, and the blue Manhattan plot shows the results of prostate cancer versus controls. The *y*-axis is the logBF (log Bayes factor) for the respective disease, the significant SNPs are highlighted in yellow, and their size is relative to the odds ratio as seen in the legend. Bottom panel: Bokeh plot of multinomial GWAS comparing AD and breast cancer in the discovery stage. The purple Manhattan plot shows the results from AD versus control, and the pink Manhattan plot shows the results of breast cancer versus controls. The *y*-axis is the logBF (log Bayes factor) for the respective disease, the significant SNPs are highlighted in yellow, and their size is relative to the odds ratio as seen in the legend. (Note: Bokeh plots are an intersection between Manhattan and bubble plots)

region had a slightly higher combined annotation-dependent depletion (CADD) score—rs4565101 had a score of 7.741, and rs58262946 at 6.342—suggesting that these SNPs are potentially deleterious.

In the regional B-GWAS of AD and breast cancer on chromosome 19, the significant SNPs mapped to *PVRL2, CTB-129P6.4, TOMM40, APOE, APOC1, APOC2, APOC4, APOC4-APOC2, CTB-129P6.11, CLPTM1, RELB, AC005779.1, MARK4, AC006126.3,* and *AC005779.2,*

and their functional annotation identified *BCAM, ZNF107, ZNF92,* and *ZNF138* (Supplementary file2). SNPs in the chromosome 5 risk region are intergenic to *FSTL4* and *VDAC1*. Other genes within 300 kb include *TCF7, SKP1, PPP2CA, CDKL3,* and *UBE2B*. The top significant SNP—rs17700949—had a CADD score of 4.224, genome-wide annotation of variants (GWAVA) score of 0.53, and regulatory Mendelian mutation (ReMM) score of 0.603, indicating a slightly deleterious effect.
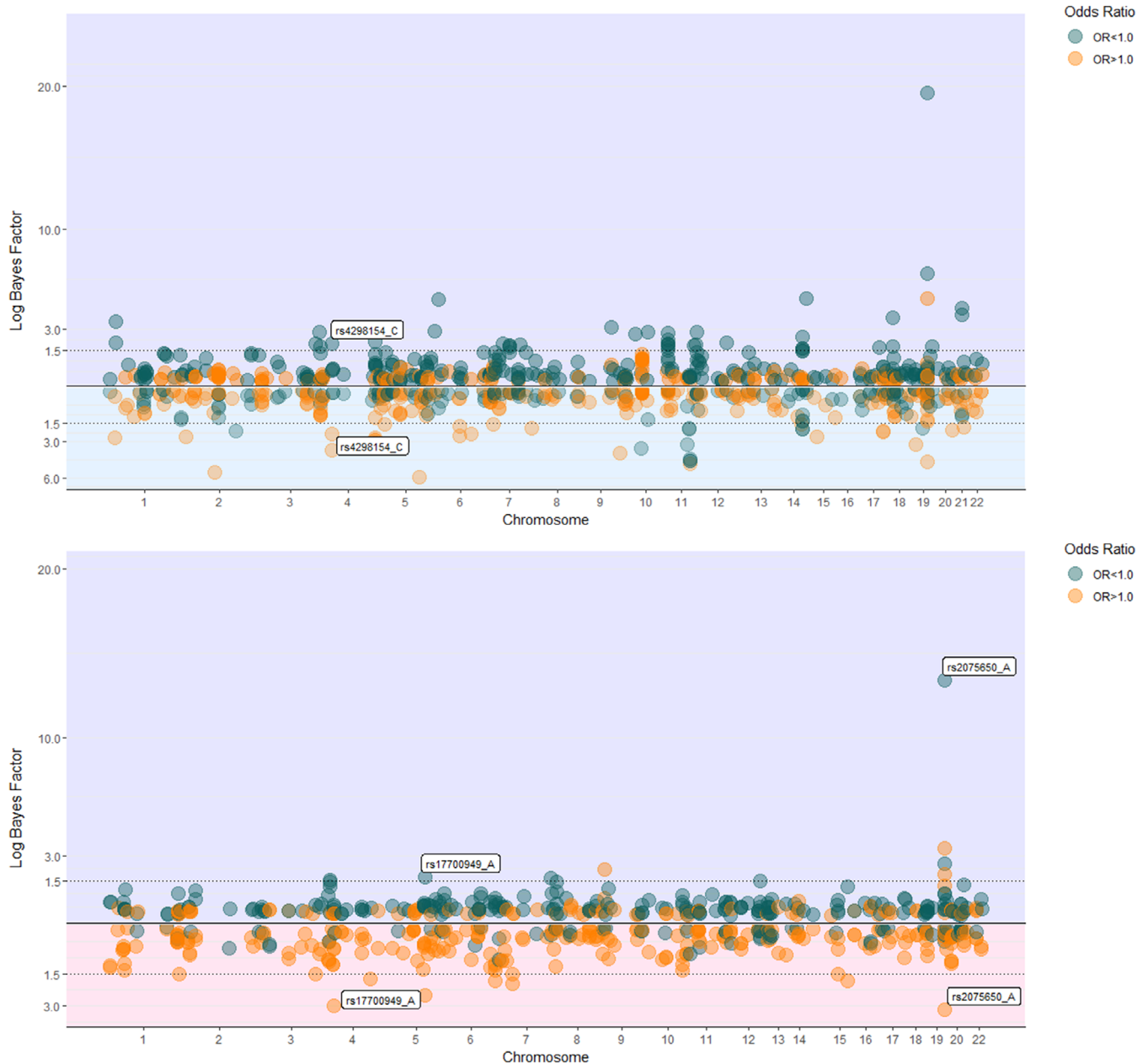
FIGURE 2 Replication stage B-GWAS results. Top panel: Bokeh plot of replication stage—multinomial GWAS comparing Alzheimer's disease (AD) and prostate cancer. Out of the 391 SNPs identified in the discovery stage based on the criteria for inverse and significant (ie, as OR < 1 for Alzheimer's and OR > 1 for cancer, or vice versa and an overall log Bayes factor of ≥ 3), 381 were typed in the replication dataset. Organized by chromosome, the log Bayes factor for the analysis comparing AD to the common controls are shown in the upward facing Manhattan plot (shaded in light purple), and the log Bayes factor for the analysis comparing prostate cancer to the common controls are shown in the downward facing Manhattan plot (shaded in light blue). One SNP from the discovery set was replicated based on inverse risk and strength of association, each indicated by the labeled data points: rs4298154. Bottom panel: Bokeh plot of replication stage—multinomial GWAS comparing AD and breast cancer. Out of the 287 SNPs identified in the discovery stage based on the criteria for inverse and significant (ie, as OR < 1 for Alzheimer's and OR > 1 for cancer, or vice versa and an overall log Bayes factor of ≥ 3), 274 were typed in the replication dataset. Organized by chromosome, the log Bayes factor for the analysis comparing AD to the common controls are shown in the upward facing Manhattan plot (shaded in light purple), and the log Bayes factor for the analysis comparing breast cancer to the common controls are shown in the downward facing Manhattan plot (shaded in light pink). Two SNPs from the discovery set were replicated based on inverse risk and strength of association, each indicated by the labeled data points: rs17700949 and rs2075650
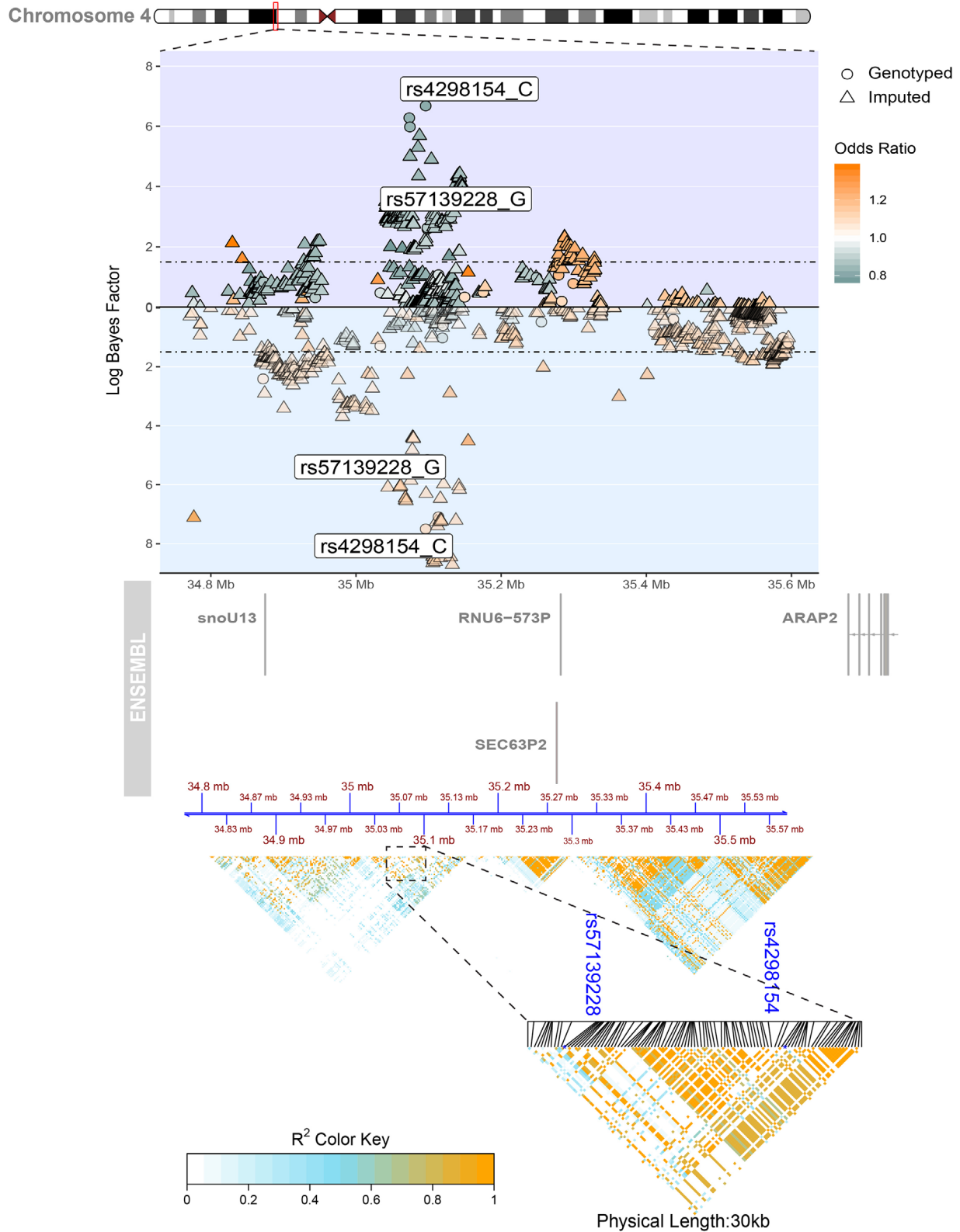
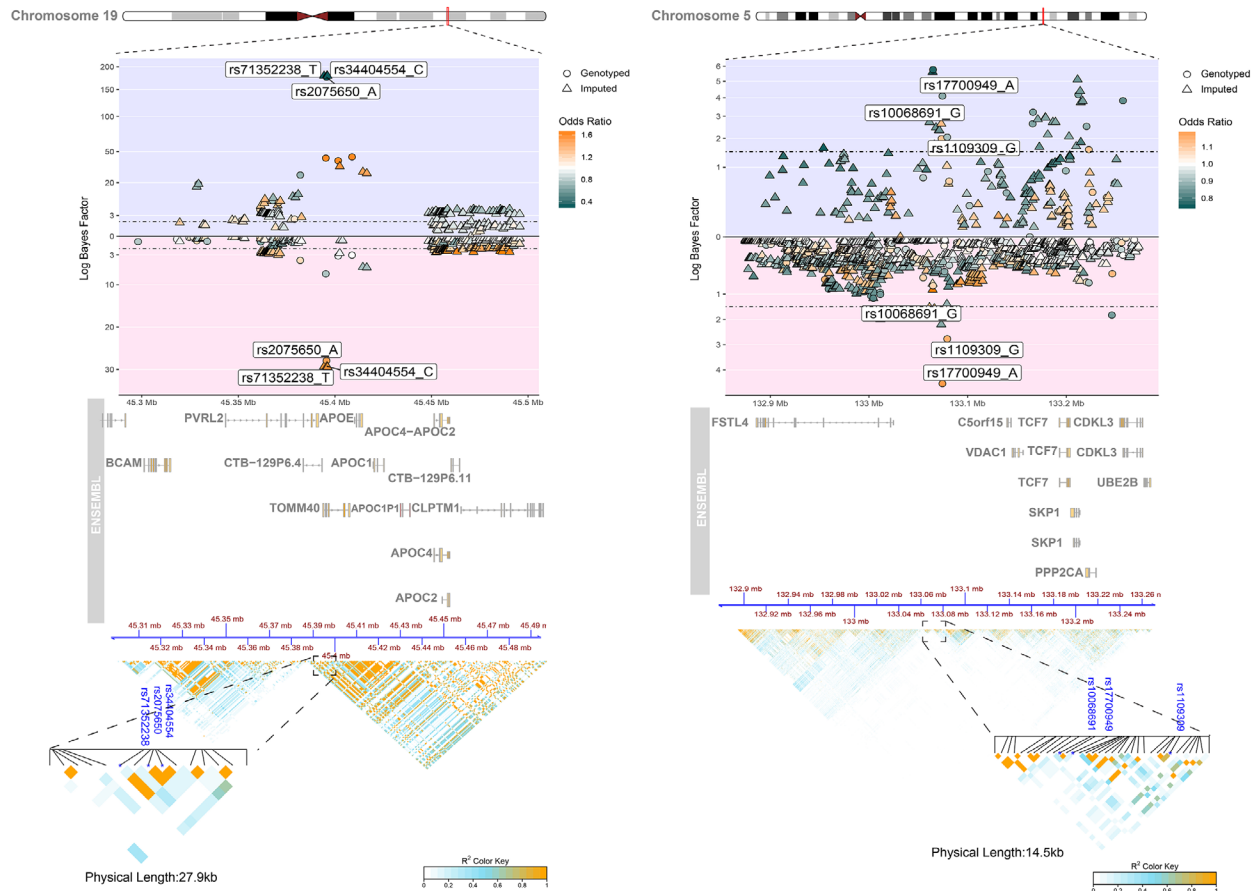**FIGURE 3** Regional Manhattan plot of chromosome 4 risk region for association between males of Alzheimer's disease (AD) and prostate cancer. Left panel: In the Manhattan plot, the purple background shows the logBF (log Bayes factor) for AD, and the blue background for prostate cancer. A total of 21 SNPs were found to be significant in the 1Mbp−chr4 risk region; the plot highlights the most significant hits within the region. The genomic coordinates are shown using GRCh37 from Ensembl, following the LD heat map of the corresponding region in the bottom panel. A zoomed-in LD map around the significant variants is shown at the bottom. Right panel: After conditioning on two SNPs with highest logBF, none of the variants were significant for both AD and cancer with opposite odds ratios

FIGURE 4   Regional Manhattan plot. Left panel: Chromosome 19 risk region for association between females of Alzheimer's disease (AD) and breast cancer. In the Manhattan plot, the purple background shows the logBF (log Bayes factor) for AD, and the pink background for breast cancer. A total of 113 SNPs were found to be significant in the 1Mbp—chr19 risk region; the plot highlights most significant hits within the region. The genomic coordinates are shown using GrCh37 from Ensembl, following the LD heat map of the corresponding region in the bottom panel. A zoomed-in LD map around the significant variants is shown at the bottom. Right panel: Regional Manhattan plot of chromosome 5 risk region for association between females of AD and breast cancer. In the Manhattan plot, the purple background shows the logBF (log Bayes factor) for AD, and the pink background for breast cancer. Three SNPs were found to be significant in the 1Mbp—chr5 risk region and highlighted in the plot. The genomic coordinates are shown using GrCh37 from Ensembl, following the LD heat map of the corresponding region in the bottom panel. A zoomed-in LD map around the significant variants is shown at the bottom

3.3 | Gene network analysis using ingenuity pathway analysis

We analyzed the query genes to test for enriched processes using IPA's biobase knowledge. Some of the represented processes were inflammatory and cellular interactions, including LXR/RXR activation, Wnt/β-catenin, PI3K/Akt, and sirtuin signaling pathway (Supplementary file3 FigureS3 in supporting information). The query genes resulted in two networks (Supplementary file3 FigureS4 in supporting information); we merged the networks and examined for leading canonical pathways (Figure 5).
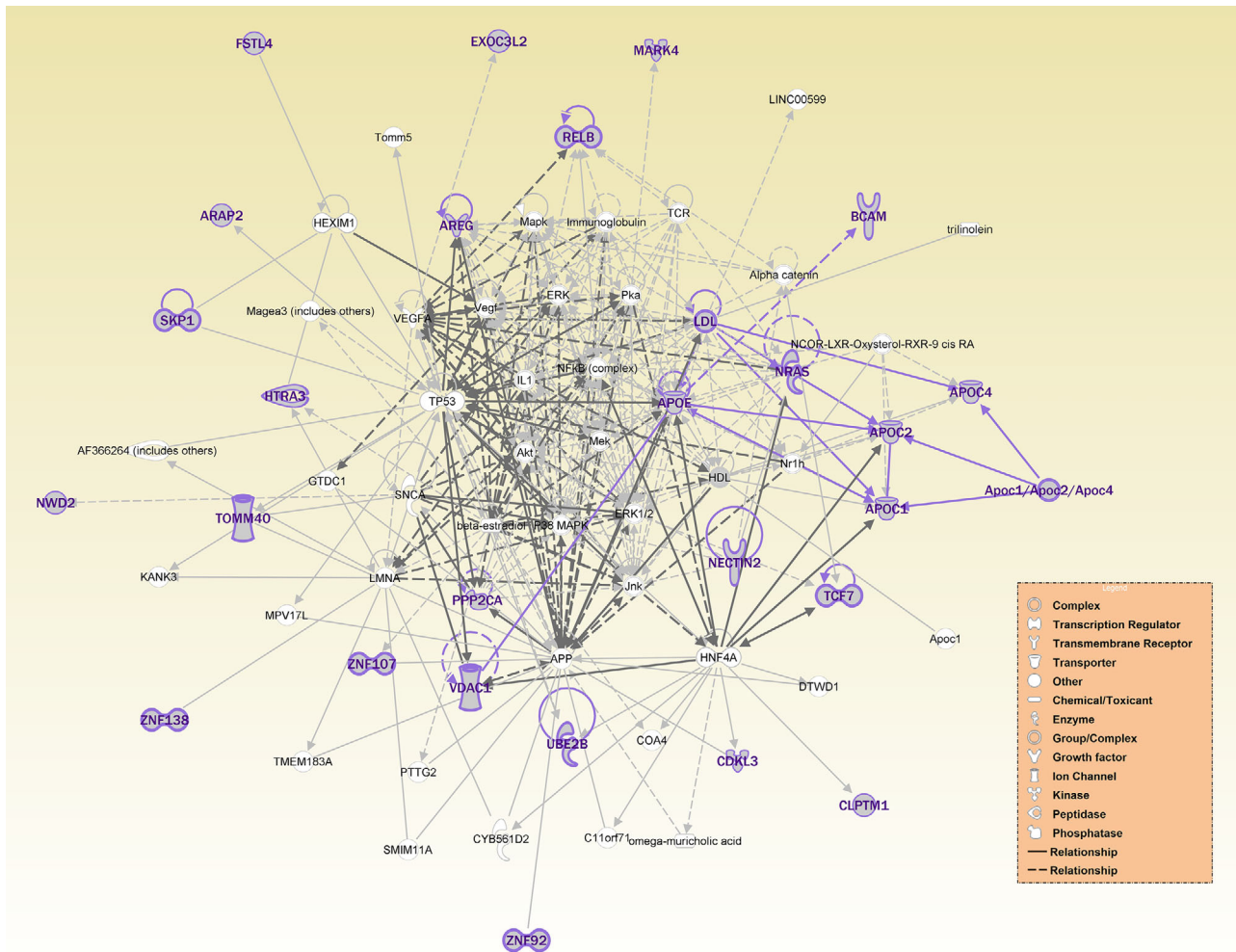
3.4 | miRNA annotation and enrichment analysis

We used the query genes to identify interacting miRNAs; the network was constructed using miRNet[25] (Figure 6). All the miRNAs in the network were assessed for miRNA family enrichment; we observed miR-515 (15 members) and miR-17 family (six members—miR-17, 20a, 20b 106a, 106b, and 93) to be significant (Supplementary file 3 Table S2). The miRNAs with the highest number of interactions (Supplementary file 3 Table S3) were investigated to find the direction of their expression changes in AD and cancer in the same tissue wherever possible. Intriguingly, comparing their expression direction in the same tissues, we see an inverse direction for these miRNA expression levels in the two diseases. Examining for miRNA-SNP binding site, we observed two SNPs—rs6859 and rs11556505—to disrupt binding sites for multiple miRNAs (Supplementary file 3 Table S4 & S5).

4 | DISCUSSION

Several GWAS have been conducted for AD, breast and prostate cancer and recently some meta-analyses have investigated the

FIGURE 5 IPA network based on genes identified by B-GWAS. Network created from query genes (highlighted in purple) using IPA's biobase knowledge

relationship between AD and cancer. Feng et al.[26]; Sanchez-Valle et al.[27] and Ibanez et al.[28] have reported that the genetic relationship between AD and cancer varies based on cancer subtypes. This is the first study that focuses on analyzing cross-phenotypic differences of SNPs using individual-level genotypes and targeting two most common age-associated cancers—breast and prostate cancer.

4.1 | Genic context of SNP hits in Alzheimer's disease and cancer

Because the top hits for breast cancer were in the *TOMM40/APOE* region, we conducted separate association analysis for SNPs in the *TOMM40* and *APOE* haplotypes among individuals with no missing SNPs to determine whether *TOMM40* was independent of *APOE*. After conditioning on the two *APOE* SNPs—rs429358 and rs769449—we found that *TOMM40* SNPs were either marginally significant for AD, or insignificant for both AD and cancer. Therefore, our findings indicate that the cross-phenotypic effects of SNPs exist in the *TOMM40/APOE*

region. Multiple GWAS have reported *APOE*'s association with risk for AD.[29] Intriguingly, *APOE* also has been a subject of investigation for carcinogenesis. A meta-analysis conducted by Anand et al.[30] reported a negative association between *APOE4* genotypes and the overall risk for cancer subtypes. Studies have reported that genotyping *TOMM40*'523 loci leads to a better prediction of AD over *APOE* predictions alone.[31] In cancer, *TOMM40* expression surface antigens were elevated in pancreatic cell lines, and gene expression was upregulated in ovarian cancer cell lines.[32,33] This heterogeneous phenotypic association of the *TOMM40/APOE/APOC1* region is evinced in our association for AD and cancer and is also summarized by Yashin et al.[34]

In the chromosome 19 region, we also identified SNPs within *MARK4* exhibiting an inverse relation between the two diseases. *MARK4* belongs to the microtubule affinity-regulating kinases family. *MARK4* and its family play role in phosphorylation of tau, mediated by co-expression of amyloid precursor protein (*APP*) and *MARK/Par-1*, as evidenced by their phosphorylated products in granulovacuolar bodies in brain tissues of AD patients.[35] In cancer, elevated *MARK4* expression is found to be correlated with cancer severity in breast,
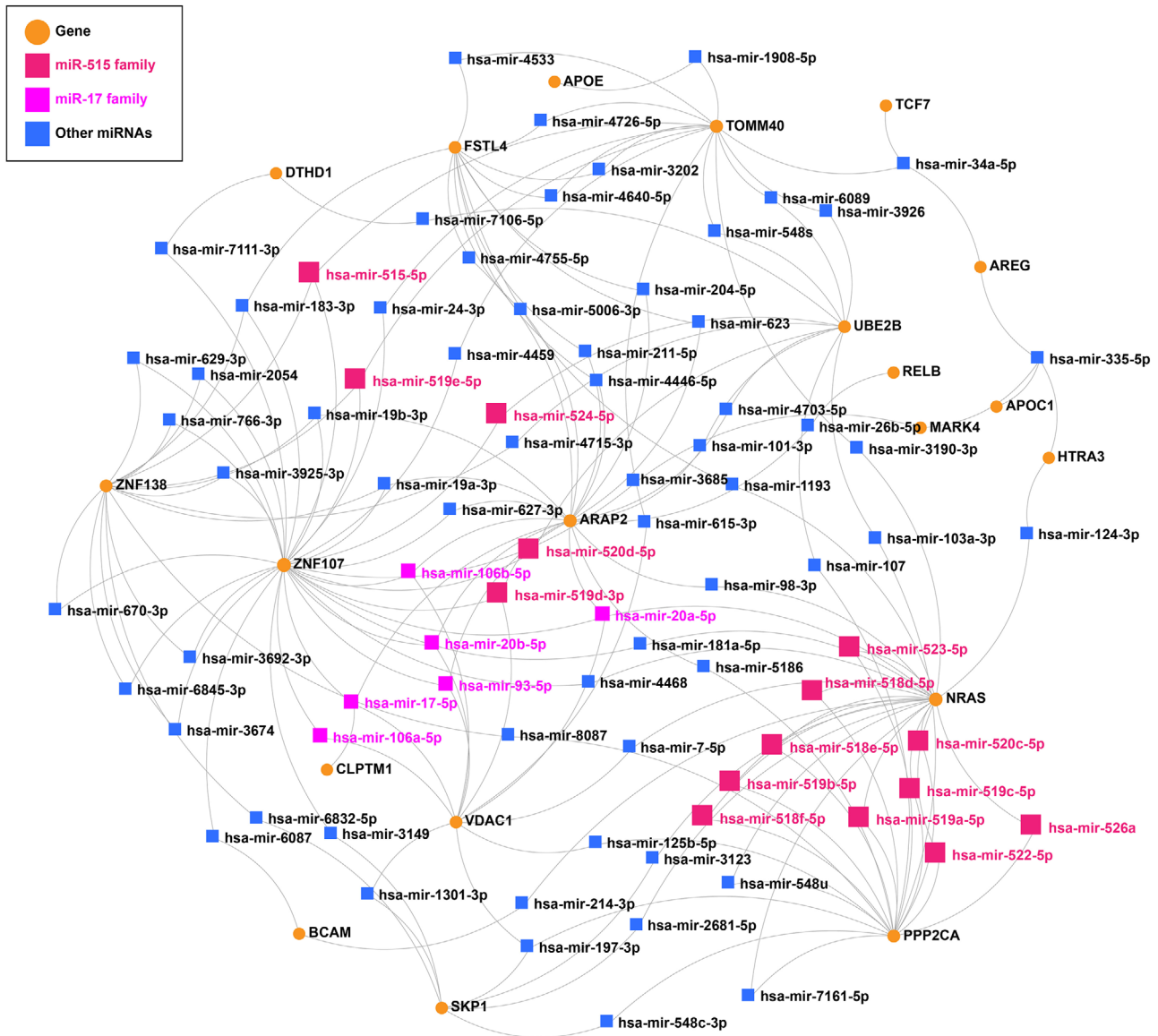
FIGURE 6 miRNA network based on genes identified by B-GWAS. The miRNA network was generated from a list of all implicated genes/loci identified in the B-GWAS; orange nodes are genes which are targeted by common miRNAs. Statistical enrichment of multiple family miRNAs was observed (dark blue squares), and several miRNAs exhibit high connectivity. Two miRNA families—miR-515 (dark pink squares) and miR-17 (magenta squares)—show statistical enrichment

lung, and prostate neoplasms[36] mediating via the upregulation of the Wnt signaling and negative regulation of mTORC. Elevated *MARK4* has also been shown to stimulate tumorigenic properties in breast cancer cells by impeding Hippo signaling.[37] Another neighboring gene—cleft lip and palate associated transmembrane protein 1 (*CLPTM1*)—in this region was recently found to be independently associated with AD in a GWAS-derived expression study.[38] An interesting finding here was that *CLPTM1L/CRR9*, a paralogue of *CLPTM1*, is widely attributed as a risk factor for multiple cancer subtypes as informed by genome-wide association and experimental studies.[39–41] Inoue et al. detected elevated expression of both *CLPTM1* and *CRR9* in oral squamous cancer cells.[39] *APOC1* in this region is associated with the formation of amyloid beta (Aβ) plaques in AD and is underexpressed in subjects with *APOE4* genotype.[42] Conversely, *APOC1* is overexpressed

in cancer tissues and influences the MAPK pathway triggering cellular expansion and motility.[43] *RELB* expression is correlated with tumor development and inflammatory processes[44] and the cumulative effect of rare variants in *RELB* is associated with amyloid burden in the cortical region of AD patients.[45]

In the chromosome 4 risk region, the top variants are intergenic and the nearest pseudogene SEC63 homolog (*Saccharomyces cerevisiae*)—pseudogene 2 (*SEC63P2*)—has been associated with coronary artery calcification[46] and body mass index.[47] The closest ($\approx$850 KB) coding gene to this region is *ARAP2*. Expression of *ARAP2* also has been reported as part of a risk score prediction for pancreatic cancer by Liu et al.[48] Variants in *ARAP2* are known to be *TP53* binding sites, and are associated with advanced prostate cancer.[49] Experimental studies have highlighted the role of *ARAP2* in cytoskeleton remodeling

and axonal transport mediated by neurotoxin stress and dysregulating motor neurons.[50]

Other loci implicated in inverse risk for breast cancer and AD are mapped between *FSTL4* and *VDAC1* on chromosome 5 using GrCh37 build. *VDAC1* is a key mitochondrial-mediated apoptotic protein that acts via the BCL-2 pathway; *VDAC1* also interacts with *TOMM40* for mitochondrial transport in the *PINK-1/PARK* pathway. In AD brain tissue, higher *VDAC1* expression is found in neurites with Aβ deposits.[51] In cancer, metabolic reprogramming has been attributed to *VDAC1*, and its apoptotic properties have become a pharmacological target of interest.[52] The upstream gene to our significant variants was *FSTL4*, known for its role in extracellular calcium ion binding. Interestingly, in the latest genome build—GRCh38—our significant variants are mapped to the *FSTL4* gene. Genome-wide studies have reported variants in this gene to be associated with lung carcinoma,[53] cognitive impairment,[54,55] and hypertension.[56]

Overall, the genes containing the cross-phenotypic SNPs have known pathological roles in both AD and cancer.

4.2 | Role of enriched processes in Alzheimer's disease and cancer

The enriched biologic processes involved with our query genes were sirtuin pathway, Wnt-signaling, liver X receptor-retinoid X receptor (LXR-RXR), and PI3K/Akt mechanism. Our findings are consistent with Ibanez et al., who reported dysregulation in Wnt-signaling—upregulation in cancer, and downregulation in neurological diseases. Wnt-signaling is implicated in metastatic cell proliferation.[28] The PI3K/Akt signaling is associated with metabolic dysfunction inducing insulin stress via deregulation of insulin receptors. While cancer cells are suspected to thrive on glycolytic byproducts from insulin stress, the brain is affected by the disturbances in PI3K/Akt signaling and exhibits cognitive deficits.[57] LXR-RXR are a class of transcription factors that also affect metabolic activity by regulating lipids and inflammatory responses.[58] Their expression in AD animal models has been associated with cognitive deficits and increased Aβ levels in cerebrospinal fluid.[58] In cancer, LXR ligands interact with both Wnt and Akt signaling pathways and induce pyroptosis—inflammation-induced cell death.[59] Sirtuin proteins are involved in both cancer and AD probably due to their involvement in regulating mitochondrial biogenesis, interacting with *TOMM40* and *VDAC1*, and can detect peripheral metabolic dysregulation.[60] Altogether, the observed processes seem to regulate metabolic activities of metastatic cellular expansion and accumulation of amyloid burden in cancer and AD, respectively.

4.3 | Inverse expression of miRNAs and their role in Alzheimer's disease and cancer

To investigate the potential mechanisms that underlie the observed genetic associations with inverse risk of AD and cancer, we turned our focus to a genetic-based regulatory system—miRNAs.[61] This provided the rationale for asking the following question: could the inverse effect of the genetic variants be due to miRNA-mediated differential regulation of our candidate genes?

miRNAs are small non-coding RNA molecules that target multiple regions in a gene and are expected to regulate ≈60% of transcripts; thus, altering cellular metabolism. Due to their exosomal packaging, they allow cross-talk through the blood–brain barrier and interact with other organs.[62] The reported genes are primarily targeted by select miRNAs including the miRNA-17 and 515 cluster, 125b, 335, and 26b, which are differentially expressed in AD and cancer (Table 1). This SNP–miRNA relationship highlights the role of these miRNAs in altering regulation of target regions identified from our study in AD. The miRNA-17 cluster (including miRNA-106, 20, and 93) has been reported to regulate *APP* expression in brain and neuronal cells of sporadic AD patients.[63] Additionally, miRNA-106 is downregulated in the frontal cortex of AD patients, which increases Aβ1-42 and induces tau phosphorylation.[64] As underscored in our results (Table 1), members of this "onco-miR"[65] family show inverse expression in the setting of AD versus cancer. The MiR-515 family was also found to be enriched in our network. The upregulation of miR-515 in cancer is inversely correlated with survival of cancer patients.[66] The miR-515 suppresses p21, which is required for inducing senescence, which is also modulated by miR-106b's overexpression.[67] MiR-515 has been reported to be downregulated in the temporal cortex of AD patients.[68] The upregulation of miR-125b in multiple regions of the AD brain has been known to correspond with neurofibrillary tangles, primarily in the gray matter region of *post-mortem* AD brains.[69] In human neuronal cells, activation of NF-κB pathways from deposition of Aβ results in overexpression of miR-125b.[70] On the other hand, 125b is underexpressed in cancer cells, which initiates cancer hallmarks.[71] 125b has also been observed to target BCL-2 and increase its apoptotic activity via BMF in AD.[69] miR-335 is found to be underexpressed in multiple cancers, which is regulated in a cyclical mode by p53.[72] In contrariety, upregulation of miR-335 triggers p21 and lowers p53 expression, which leads to increases in tau levels in AD patients.[73,74] In a mouse model of AD, miR-335 was overexpressed in the hippocampus and lowering its expression was demonstrated to reduce cellular cholesterol and alleviate cognitive impairment.[75] The upregulation of miR-26b triggers expression of cyclin-dependent kinase 5, which initiates phosphorylation of tau and apoptosis in AD.[76] Conversely, increasing 26b results in anti-tumorigenic properties.[77] Multiple cancer types have been found to have underexpression of miR-26b.[78] miR-34a has been reported to be over expressed in brain regions of AD possibly resulting in dysregulation of synaptic and metabolic activity.[79] The dysfunction of p53 governs the expression of miR-34a[80] which is deficient in most cancers.[81] In animal models of APP and presenilin 1 knockout, lowering miR-34a mitigates cognitive symptoms of AD.[82]

Overall, the identified miRNAs play a dominant role in AD pathology and their targets reported here warrant functional studies to characterize their sequence-specific multi-gene regulation.

TABLE 1 miRNAs expression in Alzheimer's disease and cancer. (References in supplementary file 3 Table S1)

miRNA	Cancer	Tissue [Ref]	Alzheimer's disease	Tissue [Ref]
hsa-miR-335	Downregulated	Serum[1] Plasma[2] Tumor[3]	Upregulated	Serum[4] Aged astrocytes and hippocampal brain[5]
hsa-miR-197	Upregulated	Tumor[6]	Downregulated	Serum[7]
	Downregulated	Tumor[8,9]	Upregulated	Cortex, CSF[10]
hsa-miR-125b	Upregulated	Tumor[11,12], serum[13], plasma[14]	Downregulated	Serum[15,16]
	Downregulated	Tumor[17,18]	Upregulated	CSF,[19] frontal cortex[20]
hsa-miR-26b	Downregulated	Tumor[21,22] Serum[23]	Upregulated	Serum[24]
hsa-miR-17	Upregulated	Serum[25]	Downregulated	Blood[29]
hsa-miR-20a	Upregulated	Tumor[30]	Downregulated	Brain[31]
hsa-miR-20b	Downregulated	Tumor[32,33]	Upregulated	Serum[34]
hsa-miR-106b	Upregulated	Tumor[35]	Downregulated	Cortex[36]
	Downregulated	Serum[37]	Upregulated	Serum[38]
hsa-miR-93	Upregulated	Tumor[35,39], serum[39]	Downregulated	Serum[40]
hsa-miR-515	Upregulated	Tumor cell line[41]	Downregulated	Brain[42]
hsa-miR-34a	Downregulated	Tumor[43]	Upregulated	Brain[44]
hsa-miR-143	Downregulated	Tumor, cell line[45]	Upregulated	Brain[46]

4.4 | Role of SNPs in disrupting miRNAs and their target binding sites

Our analyses provide evidence of potential connections between miRNAs and genetic variants resulting in bidirectional effects between AD and cancer. Studies have shown that variants present in the 3'untranslated region (3'UTR) of mRNAs, known as poly-miRTs, change the half-life of mRNAs, and thus, alter protein expression.[83] Two of our reported cross-phenotypic SNPs—rs6859 (*PVLR2/NECTIN2*) and rs11556505 (*TOMM40*)—alter miRNA binding sites. SNP rs6859 is found to alter binding site for miRNAs 143, 147, 199, 584, and 648. The elevation of miRNA-143 reduces glucose uptake and promotes cellular apoptosis in cancer cells.[84] However, in AD, the elevation of miR-143 is localized in neurons and is proportional to Braak stages of neurofibrillary tangles in the locus coeruleus region of AD brains.[85] Other miRNAs—147, 199, and 584—are understudied in AD, but share a common function of suppressing the tumor and inhibiting cancer progression.[86–88] This demonstrates that a single nucleotide variation can alter sites for multiple miRNAs leading to variability in gene expression. Using polymiRTs database,[89] rs11556505 is documented to modify miRsite for miR-484 (Supplementary file 3 Table S5). Among several targets, miR-484 is reported to inversely alter *Fis1* expression that promotes mitochondrial fission.[90] *Fis1* interacts with sirtuin complex to trigger cell migration and invasion, and is overexpressed in cancer.[91] In AD brain–derived fibroblasts and hippocampal tissue, mitochondrial fission proteins including *Fis1* are upregulated.[92] While the exact underpinnings of the interaction of *Fis1* on the reported *TOMM40* site are unknown, we observe a common thread of mitochondrial dysregulation and sirtuin signaling leading to neuronal dysfunction and cancer expansion. Therefore, this site necessitates

functional studies using whole-genome and RNA sequencing to evaluate allele-specific expression of the reported SNP-miRNA-target site.

In conclusion, the induction of SNPs within and around these UTR sequences can have multiple functional consequences by altering miRNA binding sites, generating multiple transcripts which may be differentially targeted by miRNA regulators.[93] Variants in mRNA binding sites are relatively more common than variants in genes encoding miRNAs.[94] Our analysis identified SNPs that are indicative of causing possible perturbations in miRNA binding sites. MiRNAs, either acting individually or in combination, can thus result in differential transcriptional regulation of multiple genes (Supplementary file3 Figure S5 in supporting information). While we do not know the exact mechanisms that lead to perturbations in gene expression from intergenic SNPs, studies have shown that SNPs in non-coding regions such as introns, lncRNAs, and intragenic regions can affect miRNA expression levels.[95] Recent studies have identified the importance of these reported miRNAs either via literature-driven studies or meta-analyses.[96,97] However, by studying individual SNP effects between AD and cancer, we identified targets of the mentioned miRNAs. Changes in miRNA binding site due to SNPs can be compensated by redundancy in miRNA targeting (ie, another miRNA can target site as a result of base change), which depends on codon degeneracy.[98] For instance, some members of miR-17 and miR-515 family have similar seed sequences—"AAGUGC."[99]

SNPs and miRNAs have immense potential in serving as genetic and blood-based biomarkers for diagnostic purposes, and further understanding the role of genetic predisposition will require studies of both cis and trans SNP effects. The genetic risk factors and associated miRNAs identified here would ideally be validated in a cross-conditional cohort of AD and cancer using microarray/RNA-seq

to identify functional consequences of the SNPs implicated here that exert cross-phenotypic effects between AD and cancer. Overall, these miRNAs play contrary roles in both diseases, making it imperative to investigate the strength of these miRNAs and identified targets to observe the extent of their influence in rescuing cognitive dysfunction in AD. Our future work will investigate directionality of gene expression in AD and cancer under the influence of aggregated SNPs.

4.5 | Limitations and considerations

We attempted to restrict phenotypic and technical bias for the investigation of this complex relationship between AD and cancer; however, the following considerations are important when interpreting these results. First, due to age and sex stratification, our study is underpowered to detect all SNPs, which may be exhibiting cross-effects between the two phenotypes. Second, because the ORs reported by epidemiological findings vary substantially (even for the same cancer types), we chose to remain conservative in our selection of priors for the Bayesian approach. Third, we were not able to use APOE as a covariate in the discovery phase. The genotyping of APOE is typically conducted independent of genome-wide SNP typing for AD studies; however, genotyping of APOE is not typical of cancer genetic studies. To attempt to obtain APOE genotypes for the cancer cohorts, we relied on imputation, which was not successful for all individuals. As an alternative, we adjusted for the *APOE* SNP (rs429358) as a conditional test on merged populations for females and males in each *TOMM40* haploblock to test for independent effects between *TOMM40* and *APOE*. Additionally, conditioning enabled detection of secondary associations (if any) in a local region that may have been otherwise obscured by the *APOE* effect. Fourth, when we carried out analysis by using a relaxed threshold on age (50–90) and higher priors, we get more hits including the ones being reported here, which we presume to be false positives or age-associated and not phenotype specific. This indicates that the analysis is sensitive to cohort selection procedures and we chose a more conservative approach to mitigate these confounding factors by using a two-stage design with careful inclusion/exclusion criteria. Finally, factors such as depression, education level, and medical history are important to consider for both AD and cancer. These variables were absent from the ADGC and BPC3 datasets obtained from dbGaP; therefore, such variables remained unaccounted. Because cancer history was available for the ADNI cohort, individuals with positive cancer history were removed from analysis. For the ADGC cohort used in our analysis, National Alzheimer's Care Consortium had recorded history of cancer (absence/presence) for 12.7% of individuals. Approximately 3% (N = 62) of individuals had positive cancer history (all types considered) and were subsequently removed from analysis. Because cancer history was not available for the majority of the ADGC cohort we were unable to account for cancer history of all individuals from the ADGC cohort (details in Fig S2–Supplementary File3). This limitation certainly encourages additional, explicitly designed cohorts for future studies of Alzheimer's and cancer inverse comorbidity. We believe our study has accounted for cancer in AD as per the most recent data available resulting in valuable findings for both AD and cancer research.

CONFLICT OF INTEREST

Authors have no conflicts of interest to declare.

REFERENCES

1. Mather M, Jacobsen LA, Pollard KM. Aging in the United States. Population Bulletin: Population Reference Bureau; 2015.
2. Johnson SC, Dong X, Vijg J, Suh Y. Genetic evidence for common pathways in human age-related diseases. *Aging Cell*. 2015;14:809-817.
3. Tabares-Seisdedos R, Rubenstein JL. Inverse cancer comorbidity: a serendipitous opportunity to gain insight into CNS disorders. *Nat Rev Neurosci*. 2013;14:293-304.
4. Ma LL, Yu JT, Wang HF, et al. Association between cancer and Alzheimer's disease: systematic review and meta-analysis. *J Alzheimers Dis*. 2014;42:565-573.
5. Frain L, Swanson D, Cho K, et al. Association of cancer and Alzheimer's disease risk in a national cohort of veterans. *Alzheimers Dement*. 2017;13:1364-1370.
6. Ridge PG, Mukherjee S, Crane PK, Kauwe JS, Alzheimer's Disease Genetics Consortium. Alzheimer's disease: analyzing the missing heritability. *PLoS One*. 2013;8:e79771. https://doi.org/10.1371/journal.pone.0079771
7. Lilyquist J, Ruddy KJ, Vachon CM, Couch FJ. Common genetic variation and breast cancer risk—past, present, and future. *Cancer Epidemiol Biomarkers Prev*. 2018;27:380-394.
8. Blanco-Gomez A, Castillo-Lluva S, Del Mar Saez-Freire M, et al. Missing heritability of complex diseases: enlightenment by genetic variants from intermediate phenotypes. *Bioessays*. 2016;38:664-673.
9. Morris AP, Lindgren CM, Zeggini E, et al. A powerful approach to subphenotype analysis in population-based genetic association studies. *Genet Epidemiol*. 2010;34:335-343.
10. Siegel RL, Miller KD, Jemal A. Cancer statistics, 2017. *CA Cancer J Clin*. 2017;67:7-30.
11. Wakefield J. Bayes factors for genome-wide association studies: comparison with P-values. *Genet Epidemiol*. 2009;33:79-86.
12. Burton PR, Clayton DG, Cardon LR, et al. Genome-wide association study of 14,000 cases of seven common diseases and 3,000 shared controls. *Nature*. 2007;447:661-678.
13. Spain SL, Barrett JC. Strategies for fine-mapping complex traits. *Hum Mol Genet*. 2015;24:R111-R119.
14. Majumdar A, Haldar T, Bhattacharya S, Witte JS. An efficient Bayesian meta-analysis approach for studying cross-phenotype genetic associations. *PLoS Genet*. 2018;14:e1007139.
15. Naj AC, Jun G, Beecham GW, et al. Common variants at MS4A4/MS4A6E, CD2AP, CD33 and EPHA1 are associated with late-onset Alzheimer's disease. *Nat Genet*. 2011;43:436-441.
16. Hunter DJ, Riboli E, Haiman CA, et al. A candidate gene approach to searching for low-penetrance breast and prostate cancer genes. *Nat Rev Cancer*. 2005;5:977-985.
17. Chang CC, Chow CC, Tellier LC, Vattikuti S, Purcell SM, Lee JJ. Second-generation PLINK: rising to the challenge of larger and richer datasets. *GigaScience*. 2015;4:7.
18. Anderson CA, Pettersson FH, Clarke GM, Cardon LR, Morris AP, Zondervan KT. Data quality control in genetic case-control association studies. *Nat Protoc*. 2010;5:1564-1573.
19. Zheng X, Levine D, Shen J, Gogarten SM, Laurie C, Weir BS. A high-performance computing toolset for relatedness and principal component analysis of SNP data. *Bioinformatics*. 2012;28:3326-3328.
20. Jostins L, McVean G. Trinculo: Bayesian and frequentist multinomial logistic regression for genome-wide association studies of multi-category phenotypes. *Bioinformatics*. 2016;32:1898-1900.
21. Alexander DH, Novembre J, Lange K. Fast model-based estimation of ancestry in unrelated individuals. *Genome Res*. 2009;19:1655-1664.
22. Wakefield J. Reporting and interpretation in genome-wide association studies. *Int J Epidemiol*. 2008;37:641-653.
23. Howie BN, Donnelly P, Marchini J. A flexible and accurate genotype imputation method for the next generation of genome-wide association studies. *PLoS Genet*. 2009;5:e1000529.
24. Dayem Ullah AZ, Oscanoa J, Chelala C, Nagano A, Wang J, Lemoine NR. SNPnexus: assessing the functional relevance of genetic variation to facilitate the promise of precision medicine. *Nucleic Acids Res*. 2018;46:W109-W113.
25. Ribeiro P, Arora SK, Fan Y, Xia J, Siklenka K, Kimmins S. miRNet – dissecting miRNA-target interactions and functional associations through network-based visual analysis. *Nucleic Acids Res*. 2016;44: W135-W141.
26. Feng Y-CA, Cho K, Lindstrom S, Kraft P, Cormack J, IGAP Consortium, Colorectal Transdisciplinary Study (CORECT), et al. Investigating the genetic relationship between Alzheimer's disease and cancer using GWAS summary statistics. *Hum Genet* 2017;136:134-151. https://doi.org/10.1007/s00439-017-1831-6
27. Sánchez-Valle J, Tejero H, Ibáñez K, Portero JL, Krallinger M, Al-Shahrour F, et al. A molecular hypothesis to explain direct and inverse co-morbidities between Alzheimer's Disease, Glioblastoma and Lung cancer. *Sci Rep* 2017;7:4474. https://doi.org/10.1038/s41598-017-04400-6
28. Ibanez K, Boullosa C, Tabares-Seisdedos R, Baudot A, Valencia A. Molecular evidence for the inverse comorbidity between central nervous system disorders and cancers detected by transcriptomic meta-analyses. *PLoS Genet*. 2014;10:e1004173.
29. Riedel BC, Thompson PM, Brinton RD. Age, APOE and sex: triad of risk of Alzheimer's disease. *J Steroid Biochem Mol Biol*. 2016;160:134-147.
30. Anand R, Prakash SS, Veeramanikandan R, Kirubakaran R. Association between apolipoprotein E genotype and cancer susceptibility: a meta-analysis. *J Cancer Res Clin Oncol*. 2014;140:1075-1085.
31. Roses A, Sundseth S, Saunders A, Gottschalk W, Burns D, Lutz M. Understanding the genetics of APOE and TOMM40 and role of mitochondrial structure and function in clinical pharmacology of Alzheimer's disease. *Alzheimers Dement*. 2016;12:687-694.

32. Kim S, Cho H, Yang W, et al. Abstract 2456: overexpression of TOM40 (translocase in the outer mitochondrial membrane 40) inhibits the cell proliferation, invasion and migration abilities in ovarian cancer cell lines. *Mol Cell Biol.* 2014;74.

33. Ning L, Pan B, Zhao Y-P, et al. Immuno-proteomic screening of human pancreatic cancer associated membrane antigens for early diagnosis. *Zhonghua Wai Ke Za Zhi.* 2007;45:34-38.

34. Yashin AI, Fang F, Kovtun M, et al. Hidden heterogeneity in Alzheimer's disease: insights from genetic association studies and other analyses. *Exp Gerontol.* 2018;107:148-160.

35. Annadurai N, Agrawal K, Džubák P, Hajdúch M, Das VJC, Sciences ML. Microtubule affinity-regulating kinases are potential druggable targets for Alzheimer's disease. *Cell Mol Life Sci.* 2017;74:4159-4169.

36. Jenardhanan P, Mannu J, Mathur PP. The structural analysis of MARK4 and the exploration of specific inhibitors for the MARK family: a computational approach to obstruct the role of MARK4 in prostate cancer progression. *Mol Biosyst.* 2014;10:1845-1868.

37. Heidary Arash E, Shiban A, Song S, Attisano L. MARK4 inhibits Hippo signaling to promote proliferation and migration of breast cancer cells. *EMBO Rep.* 2017;18:420-436.

38. Hao S, Wang R, Zhang Y, Zhan H. Prediction of Alzheimer's disease-associated genes by integration of GWAS summary data and expression data. *Front Genet.* 2019;9:653.

39. Inoue K, Hatano K, Hanamatsu Y, et al. Pathobiological role of cleft palate transmembrane protein 1 family proteins in oral squamous cell carcinoma. *J Cancer Res Clin Oncol.* 2019;145:851-859.

40. Yang YC, Fu WP, Zhang J, Zhong L, Cai SX, Sun C. rs401681 and rs402710 confer lung cancer susceptibility by regulating TERT expression instead of CLPTM1L in East Asian populations. *Carcinogenesis.* 2018;39:1216-1221.

41. Koike Folgueira MAA, Carraro DM, Brentani H, et al. Gene expression profile associated with response to doxorubicin-based therapy in breast cancer. *Clin Cancer Res.* 2005;11:7434-7443.

42. Cudaback E, Li X, Yang Y, et al. Apolipoprotein C-I is an APOE genotype-dependent suppressor of glial activation. *J Neuroinflammation.* 2012;9:192.

43. Ren H, Chen Z, Yang L, et al. Apolipoprotein C1 (APOC1) promotes tumor progression via MAPK signaling pathways in colorectal cancer. *Cancer Manag Res.* 2019;11:4917-4930.

44. Giopanou I, Lilis I, Papadaki H, Papadas T, Stathopoulos GT. A link between RelB expression and tumor progression in laryngeal cancer. *Oncotarget.* 2017;8:114019-114030.

45. Nho K, Kim S, Horgusluoglu E, et al. Association analysis of rare variants near the APOE region with CSF and neuroimaging biomarkers of Alzheimer's disease. *BMC Med Genomics.* 2017;10:29.

46. Divers J, Palmer ND, Langefeld CD, et al. Genome-wide association study of coronary artery calcified atherosclerotic plaque in African Americans with type 2 diabetes. *BMC Genet.* 2017;18:105.

47. Melen E, Granell R, Kogevinas M, et al. Genome-wide association study of body mass index in 23 000 individuals with and without asthma. *Clin Exp Allergy.* 2013;43:463-474.

48. Liu Y, Zhu D, Xing H, Hou Y, Sun Y. A 6-gene risk score system constructed for predicting the clinical prognosis of pancreatic adenocarcinoma patients. *Oncol Rep.* 2019;41:1521-1530.

49. Lin VC, Huang C-Y, Lee Y-C, et al. Genetic variations in TP53 binding sites are predictors of clinical outcomes in prostate cancer patients. *Arch Toxicol.* 2014;88:901-911.

50. Boutahar N, Wierinckx A, Camdessanche JP, et al. Differential effect of oxidative or excitotoxic stress on the transcriptional profile of amyotrophic lateral sclerosis-linked mutant SOD1 cultured neurons. *J Neurosci Res.* 2011;89:1439-1450.

51. Shoshan-Barmatz V, Nahon-Crystal E, Shteinfer-Kuzmine A, Gupta R. VDAC1, mitochondrial dysfunction, and Alzheimer's disease. *Pharmacol Res.* 2018;131:87-101.

52. Mazure NM. VDAC in cancer. *Biochim Biophys Acta Biomembr.* 2017;1858:665-673.

53. McKay JD, Hung RJ, Han Y, et al. Large-scale association analysis identifies new lung cancer susceptibility loci and heterogeneity in genetic susceptibility across histological subtypes. *Nat Genet.* 2017;49:1126.

54. Liu C, Chyr J, Zhao W, et al. Genome-wide association and mechanistic studies indicate that immune response contributes to Alzheimer's disease development. *Front Genet.* 2018;9:410.

55. Warrier V, Grasby KL, Uzefovsky F, et al. Genome-wide meta-analysis of cognitive empathy: heritability, and correlates with sex, neuropsychiatric conditions and cognition. *Mol Psychiatry.* 2017;23:1402.

56. Guo Y, Tomlinson B, Chu T, et al. A genome-wide linkage and association scan reveals novel loci for hypertension and blood pressure traits. *PLoS One.* 2012;7:e31489.

57. Nudelman KNH, McDonald BC, Lahiri DK, Saykin AJ. Biological hallmarks of cancer in Alzheimer's disease. *Mol Neurobiol.* 2019;56:7173-7187.

58. Wang S, Wen P, Wood S. Effect of LXR/RXR agonism on brain and CSF Aβ40 levels in rats [version 2; peer review: 1 approved, 2 approved with reservations]. *F1000Res.* 2016;5:138. https://doi.org/10.12688/f1000research.7868.2

59. Ju X, Huang P, Chen M, Wang Q. Liver X receptors as potential targets for cancer therapeutics. *Oncol Lett.* 2017;14:7676-7680.

60. Jeśko H, Wencel P, Strosznajder RP, Strosznajder JB. Sirtuins and their roles in brain aging and neurodegenerative disorders. *Neurochem Res.* 2017;42:876-890.

61. Grasso M, Piscopo P, Confaloni A, Denti MA. Circulating miR-NAs as biomarkers for neurodegenerative disorders. *Molecules.* 2014;19:6891-6910.

62. Nagaraj S, Zoltowska KM, Laskowska-Kaszub K, Wojda U. microRNA diagnostic panel for Alzheimer's disease and epigenetic trade-off between neurodegeneration and cancer. *Ageing Res Rev.* 2019;49:125-143.

63. Basavaraju M, de Lencastre A. Alzheimer's disease: presence and role of microRNAs. *Biomol Concepts.* 2016;7:241-252.

64. Zhao J, Yue D, Zhou Y, et al. The role of microRNAs in Aβ deposition and tau phosphorylation in Alzheimer's disease. *Front Neurol.* 2017;8:342.

65. Li H, Wu Q, Li T, et al. The miR-17-92 cluster as a potential biomarker for the early diagnosis of gastric cancer: evidence and literature review. *Oncotarget.* 2017;8:45060-45071.

66. Pardo OE, Castellano L, Munro CE, et al. miR-515-5p controls cancer cell migration through MARK4 regulation. *EMBO Rep.* 2016;17:570-584.

67. Gorospe M, Abdelmohsen K. MicroRegulators come of age in senescence. *Trends Genet.* 2011;27:233-241.

68. Pichler S, Gu W, Hartl D, et al. The miRNome of Alzheimer's disease: consistent downregulation of the miR-132/212 cluster. *Neurobiol Aging.* 2017;50:167.e1-167.e10.

69. Holohan KN, Lahiri DK, Schneider BP, Foroud T, Saykin AJ. Functional microRNAs in Alzheimer's disease and cancer: differential regulation of common mechanisms and pathways. *Front Genet.* 2013;3:323.

70. Wang M, Qin L, Tang B. MicroRNAs in Alzheimer's disease. *Front Genet.* 2019;10:153.

71. Wang H, Tan G, Dong L, et al. Circulating MiR-125b as a marker predicting chemoresistance in breast cancer. *PLoS One.* 2012;7:e34210.

72. Sandoval-Bórquez A, Polakovicova I, Carrasco-Véliz N, et al. MicroRNA-335-5p is a potential suppressor of metastasis and invasion in gastric cancer. *Clin Epigenetics.* 2017;9:114.

73. Tomé M, Sepúlveda JC, Delgado M, et al. miR-335 correlates with senescence/aging in human mesenchymal stem cells and inhibits their therapeutic actions through inhibition of AP-1 activity. *Stem Cells.* 2014;32:2229-2244.

74. Szybińska A, Leśniak W. P53 dysfunction in neurodegenerative diseases–the cause or effect of pathological changes? *Aging Dis.* 2017;8:506-518.

75. Raihan O, Brishti A, Molla MR, et al. The age-dependent elevation of miR-335-3p leads to reduced cholesterol and impaired memory in brain. *Neuroscience*. 2018;390:160-173.

76. Absalon S, Kochanek DM, Raghavan V, Krichevsky AM. MiR-26b, upregulated in Alzheimer's disease, activates cell cycle entry, tau-phosphorylation, and apoptosis in postmitotic neurons. *J Neurosci*. 2013;33:14645-14659.

77. Li Y, Sun Z, Liu B, Shan Y, Zhao L, Jia L. Tumor-suppressive miR-26a and miR-26b inhibit cell aggressiveness by regulating FUT4 in colorectal cancer. *Cell Death Dis*. 2017;8:e2892.

78. Verghese ET, Drury R, Green CA, et al. MiR-26b is down-regulated in carcinoma-associated fibroblasts from ER-positive breast cancers leading to enhanced cell migration and invasion. *J Pathol*. 2013;231:388-399.

79. Sarkar S, Jun S, Rellick S, Quintana DD, Cavendish JZ, Simpkins JW. Expression of microRNA-34a in Alzheimer's disease brain targets genes linked to synaptic plasticity, energy metabolism, and resting state network activity. *Brain Res*. 2016;1646:139-151.

80. Okada N, Lin C-P, Ribeiro MC, et al. A positive feedback between p53 and miR-34 miRNAs mediates tumor suppression. *Genes Dev*. 2014;28:438-450.

81. Slabáková E, Culig Z, Remšík J, Souček K. Alternative mechanisms of miR-34a regulation in cancer. *Cell Death Dis*. 2017;8:e3100.

82. Xu Y, Chen P, Wang X, Yao J, Zhuang S. miR-34a deficiency in APP/PS1 mice promotes cognitive function by increasing synaptic plasticity via AMPA and NMDA receptors. *Neurosci Lett*. 2018;670:94-104.

83. Moszyńska A, Gebert M, Collawn JF, Bartoszewski R. SNPs in microRNA target sites and their potential role in human disease. *Open Biol*. 2017;7:170019.

84. Zhao J, Chen Y, Liu F, Yin M. Overexpression of miRNA-143 inhibits colon cancer cell proliferation by inhibiting glucose uptake. *Arch Med Res*. 2018;49:497-503.

85. Llorens F, Thune K, Andres-Benito P, et al. MicroRNA expression in the locus coeruleus, entorhinal cortex, and hippocampus at early and middle stages of braak neurofibrillary tangle pathology. *J Mol Neurosci*. 2017;63:206-215.

86. Su WZ, Ren LF. MiRNA-199 inhibits malignant progression of lung cancer through mediating RGS17. *Eur Rev Med Pharmacol Sci*. 2019;23:3390-3400.

87. Zhang Y, Wang Y, Wang J. MicroRNA-584 inhibits cell proliferation and invasion in non-small cell lung cancer by directly targeting MTDH. *Exp Ther Med*. 2018;15:2203-2211.

88. Momen-Heravi F, Trachtenberg AJ, Kuo WP, Cheng YS. Genomewide study of salivary microRNAs for detection of oral cancer. *J Dent Res*. 2014;93:86S-93S.

89. Bhattacharya A, Ziebarth JD, Cui Y. PolymiRTS Database 3.0: linking polymorphisms in microRNAs and their target sites with human diseases and biological pathways. *Nucleic Acids Res*. 2014;42:D86-D91.

90. Wang K, Long B, Jiao J-Q, et al. miR-484 regulates mitochondrial network through targeting Fis1. *Nat Commun*. 2012;3:781.

91. Williams M, Caino MC. Mitochondrial dynamics in type 2 diabetes and cancer. *Front Endocrinol (Lausanne)*. 2018;9:211.

92. Wang X, Su B, Lee H-G, et al. Impaired balance of mitochondrial fission and fusion in Alzheimer's disease. *J Neurosci*. 2009;29:9090-9103.

93. Wilk G, Braun R. regQTLs: single nucleotide polymorphisms that modulate microRNA regulation of gene expression in tumors. *PLoS Genet*. 2018;14:e1007837.

94. Saunders MA, Liang H, Li W-H. Human polymorphism at microRNAs and microRNA target sites. *Proc Natl Acad Sci U S A*. 2007;104:3300-3305.

95. Hrdlickova B, de Almeida RC, Borek Z, Withoff S. Genetic variation in the non-coding genome: involvement of micro-RNAs and long non-coding RNAs in disease. *Biochim Biophys Acta Mol Basis Dis*. 2014;1842:1910-1922.

96. Takousis P, Sadlon A, Schulz J, et al. Differential expression of microRNAs in Alzheimer's disease brain, blood, and cerebrospinal fluid. *Alzheimer's Dement*. 2019;15:1468-1477. https://doi.org/10.1016/j.jalz.2019.06.4952

97. Rahman MR, Islam T, Zaman T, et al. Blood-based molecular biomarker signatures in Alzheimer's disease: insights from systems biomedicine perspective. *bioRxiv*. 2018;481879.

98. Maleszka R, Mason PH, Barron AB. Epigenomics and the concept of degeneracy in biological systems. *Brief Funct Genomic Proteomic*. 2013;13:191-202.

99. Malnou EC, Umlauf D, Mouysset M, Cavaillé J. Imprinted microRNA gene clusters in the evolution, development, and functions of mammalian placenta. *Front Genet*. 2019;9:706.

SUPPORTING INFORMATION

Additional supporting information may be found online in the Supporting Information section at the end of the article.